Assembly of N-hexadecyl-pyridinium-4-boronic acid hexafluorophosphate monolayer films with catechol sensing selectivity. J Mater Chem

ARTICLE *in* JOURNAL OF MATERIALS CHEMISTRY · OCTOBER 2010

Impact Factor: 7.44 · DOI: 10.1039/C0JM01510E

Assembly of *N*-hexadecyl-pyridinium-4-boronic acid hexafluorophosphate monolayer films with catechol sensing selectivity

Yan-Jun Huang,[ab] Yun-Bao Jiang,[b] John S. Fossey,[c] Tony D. James[a] and Frank Marken*[a]

Received 19th May 2010, Accepted 21st July 2010
DOI: 10.1039/c0jm01510e

The highly water insoluble *N*-hexadecyl-pyridinium-4-boronic acid hexafluorophosphate is synthesised and investigated for sensor applications. This amphiphilic molecule is immobilised by evaporation of an acetonitrile solution at a basal plane pyrolytic graphite (HOPG) electrode surface and is shown to provide a monolayer film. By varying the amount of deposit partial or full coverage can be achieved. The *N*-hexadecyl-pyridinium-4-boronic acid hexafluorophosphate monolayer acts as an active receptor for 1,2-dihydroxy-benzene (catechol) derivatives in aqueous media. The ability to bind alizarin red S is investigated and the Langmuirian binding constant determined as a function of pH. It is shown that the immobilised boronic acid monolayer acts as sensor film for a wider range of catechols. A comparison of Langmuirian binding constants for alizarin red S (1.4×10^5 mol^{-1} dm^3), catechol (8.4×10^4 mol^{-1} dm^3), caffeic acid (7.5×10^4 mol^{-1} dm^3), dopamine (1.0×10^4 mol^{-1} dm^3), and L-dopa (8×10^3 mol^{-1} dm^3) reveals that a combination of hydrophobicity and electrostatic interaction causes considerable selectivity effects.

1. Introduction

Boronic acids are capable of reversible formation of strong covalent bonds with diol functionalities for example to form of 5- or 6-membered cyclic esters with carbohydrates.[1] This binding process in aqueous media is important for sensor applications and superior to other sensor systems involving weaker non-covalent or hydrogen bonded interactions. Among the diols capable of complexation with boronic acids, catechols are excellent candidates[2] due to the *syn-peri*-planar aromatic hydroxyl groups and effective π-donation. Many biologically important species contain catechol fragments, *e.g.* dopamine and caffeic acid, and therefore boronic acids immobilised on sensor surfaces are promising motifs for the detection of these molecule under physiological condition.[3,4] In aqueous media catechol can be reversibly transformed into its oxidised form 1,2-benzoquinone. The boronate esters formed by reaction of the aromatic 1,2-diol with boronic acid are electrochemically oxidised at potentials considerably more positive compared to those necessary to oxidize free catechol at pH 7.[4] An electrochemical sensor response based on surface-immobilised boronate esters is therefore expected to be distinct from the response for the free catechol.

Modified electrodes are widely used to detect analytes including metal ions,[5] DNA,[6] and saccharides.[7] Boronic acid modified electrodes have been developed based on boronic acid dendrimer nano-composites,[8] boronic acid containing micro-droplet deposits,[9] carbon nanotubes modified with boronic acids,[10] conducting polymer films,[11–13] self-assembled thiol films on gold[14,15] and on gold nanoparticles,[16] diazo-coupled phenylboronic acids,[17] boronic acid functionalised TTF[18] and glutaraldehyde coupled boronic acids[19] on glassy carbon. The potential applications of boronic acid modified electrode surfaces include the detection of glucose[20–22] other saccharides (carbohydrates),[23–34] glycosylated proteins,[35] chirality[36–44] and oxidative stress markers.[45]

Herein a novel boronic acid immobilisation strategy based on a self-assembly process on basal plane pyrolytic graphite electrode surfaces is reported. A highly hydrophobic boronic acid, *N*-hexadecyl-pyridinium-4-boronic acid hexafluorophosphate, is synthesised which is similar to boronic acid structures employed by Mohler and Czarnik that allowed transmembrane drug transport in living cells.[46] The hydrophobicity of this new boronic acid material allows facile assembly of monolayers on hydrophobic electrode surfaces with potential applications in sensors without covalent attachment. The physical monolayer attachment allows rapid renewal of the sensor film and opens up applications on many types of sensor surfaces without the need for chemical attachment.

2. Experimental details

2.1. Chemical reagents

Dopamine hydrochloride and caffeic acid were purchased from Sigma. L-Dopa, catechol, alizarin red S, 4-pyridineboronic acid were obtained from Aldrich. KPF_6 and 1-bromohexadecane were obtained from Arcos, NaH_2PO_4 obtained from Fisher, and ion-exchange resin amberlite IR-120 obtained from Merck. All reagents were of analytical purity and used without further purification.

2.2. Instrumentation

A micro-Autolab III (Ecochemie, NL) with GPES software was employed for electrochemical measurements. A KCl-saturated

[a]*Department of Chemistry, University of Bath, Claverton Down, Bath, BA2 7AY, UK. E-mail: F.Marken@bath.ac.uk*
[b]*Department of Chemistry, College of Chemistry and Chemical Engineering, and the MOE Key Laboratory of Analytical Sciences, Xiamen University, Xiamen, 361005, China*
[c]*School of Chemistry, University of Birmingham Edgbaston, Birmingham, B15 2TT, UK*

calomel electrode (SCE) and platinum wire were the reference and counter, respectively. A 4.9 mm diameter basal plane pyrolytic graphite (Pyrocarbon, Le Carbone, UK) electrode was the working electrode. The electrode surface was renewed by polishing on fine caborundum paper. Solutions were de-aerated with argon (BOC). All experiments were conducted at a temperature of 20 ± 2 °C.

2.3. Synthesis of *N*-hexadecyl-pyridinium-4-boronic acid hexafluorophosphate

4-Pyridineboronic acid (1.23 g, 10 mmol) and 2,2-dimethyl-1,3-propanediol (1.04 g, 10 mmol) were mixed in toluene (150 mL). A Dean–Stark head was fitted and the reaction mixture was heated under reflux for 3 h. The mixture was allowed to cool to room temperature. The solution was washed with water (3 × 30 mL), then dried over sodium sulfate and filtered. Volatiles were removed and resulting white solid dried *in vacuo* to yield 4-(5, 5-dimethyl-1, 3, 2-dioxanborinan-2-yl)pyridine **1** (see eqn (1)).

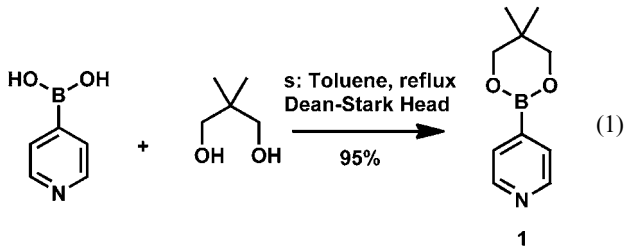

(1)

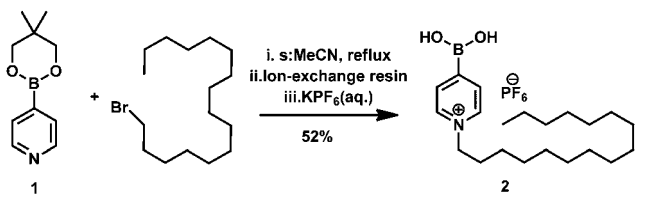

(2)

A mixture of compound **1** (96 mg, 0.5 mmol) and 1-bromohexadecane (152 mg, 0.5 mmol) in acetonitrile (10 mL) was heated at reflux for 48 h under N_2. After removal of the solvent the mixture was dissolved in MeOH and treated with ion-exchange resin, 0.2 mol L^{-1} HCl–MeOH as eluent. The boronic acid was deprotected simultaneously to give the alkyl pyridinium as a chloride salt. Dropwise addition of aqueous saturated KPF_6 solution into a methanol solution of the chloride salt formed a precipitate. After washing the precipitate several times with water, the desired product, *N*-hexadecyl-pyridinium-4-boronic acid hexafluorophosphate **2**, was obtained as a white solid in 52% yield (128 mg). ESI-MS (*m*/*z*): [M^+] calculated for $C_{21}H_{39}NO_2B$, 348.31; found 348.31. ^{1}H NMR (250 MHz methanol-d_4) δ 8.91 (d, 2H, $J = 6$ Hz), 8.27 (d, 2H, $J = 6$ Hz), 4.65 (t, 2H, $J = 7.5$ Hz), 2.06 (m, 2H), 1.31 (m, 26H), 0.95 (t, 3H, $J = 6.5$ Hz). ^{13}C NMR (300 MHz, methanol-d_4) δ 144.3, 133.5, 63.1, 33.5, 32.9, 31.2, 30.9, 30.5, 27.6, 24.2, 14.9, one carbon was not observed due to quadropolar relaxation by the boron.

2.3. Electrode modification protocol

A solution of *N*-hexadecyl-pyridinium-4-boronic acid hexafluorophosphate **2** in acetonitrile (0.2 mM concentration in a 10 mL volume) was prepared and films on the basal plane pyrolytic graphite electrode were formed by evaporation. In a typical experiment, 5 μL stock solution was evaporated onto a 4.9 mm diameter electrode to give a 1 nmol deposit (corresponding to 5.3 nmol cm^{-2}).

3. Results and discussion

3.1. *N*-Hexadecyl-pyridinium-4-boronic acid monolayer films I: binding and cathodic detection of alizarin red S

Alizarin red S is known to bind to boronic acids with a binding constant of approximately 6000 mol^{-1} dm^3 in aqueous media[8] and has often been employed as a redox probe for electrodes modified with boronic acids.[8] Herein, we report initial investigations on the binding of alizarin red S onto the bare basal plane of HOPG. Fig. 1A shows a voltammogram for a clean graphite electrode and an electrode after immersion in 1 mM alizarin red S in aqueous 0.1 M phosphate buffer pH 7. The voltammograms were recorded after transfer into clean 0.1 M phosphate buffer pH 7. Two processes due to surface adsorbed alizarin red S can be identified which correspond to the 2-electron 2-proton reduction of alizarin red S (P1, see eqn (3)) and the 2-electron 2-proton oxidation of alizarin red S (P2, see eqn (4)).

From these measurements it is apparent that alizarin red S is amphiphilic and readily adsorbed and the charge for a monolayer adsorption is approximately 40 μC (or 212 μC cm^{-2}). This

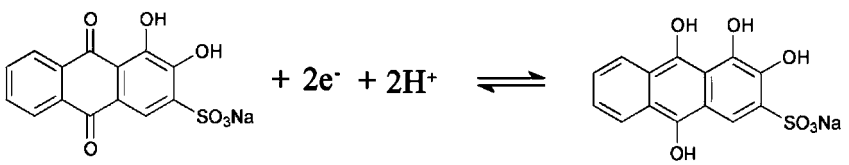

(3)

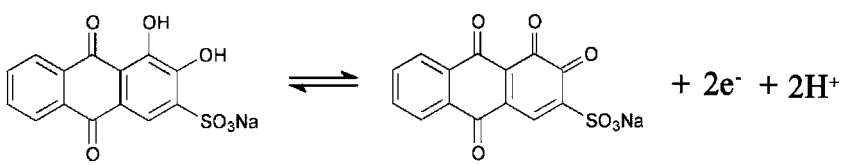

(4)

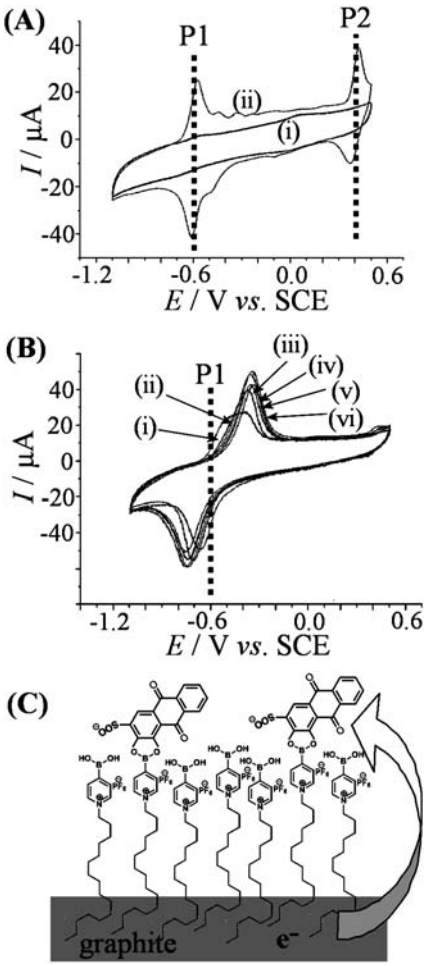

Fig. 1 (A) Cyclic voltammograms (scan rate 0.1 V s^{-1}) for alizarin red S (adsorbed from 1 mM solution in aqueous 0.1 M phosphate buffer pH 7) at a 4.9 mm diameter basal plane HOPG electrode immersed in 0.1 M phosphate buffer pH 7. (B) Conditions as in (A) but with *N*-hexadecyl-pyridinium-4-boronic acid hexafluorophosphate (i) 3×10^{-10} mol, (ii) 5×10^{-10} mol, (iii) 1×10^{-9} mol, (iv) 2×10^{-9} mol, (v) 3×10^{-9} mol, and (vi) 5×10^{-9} mol pre-deposited onto the HOPG electrode surface. (C) Schematic drawing of a graphite electrode with immobilised boronic acid film and binding to alizarin red S.

corresponds to 1.2×10^{14} molecules (0.2 nmol) on the electrode surface (corresponding to 6.4 molecules cm^{-2}) or a realistic geometric area of 4 Å × 4 Å per alizarin red S molecule at the surface of the graphite electrode (not taking into account electrode roughness).

The estimated roughness factor as given by real surface area/geometric surface area ≈ 1.4 for the graphite surface and the possible presence of different types of adsorption sites suggest a more complex surface structure and indeed additional voltammetric peaks are observed in Fig. 1A. However, throughout this report the surface will be considered flat in order to facilitate interpretation of data.

Next, the experiment was repeated but with *N*-hexadecyl-pyridinium-4-boronic acid hexafluorophosphate pre-deposited at the graphite electrode surface. It can be seen that the shape of the voltammetric response for the reduction of alizarin red S (P1) is considerably different and the voltammetric response for the oxidation of alizarin red S (P2) is suppressed (shifted positive, not shown). The new signal for the reduction of the boronic acid bound alizarin red S is fully developed with *ca.* 0.5 nmol boronic acid deposit (corresponding to 2.6 nmol cm^{-2}) and further excess of boronic acid is shown to have no effect. This amount of the boronic acid derivative is in good agreement with a monolayer at the HOPG electrode surface. The boronic acid derivative has a typical amphiphilic structure with a highly non-polar alkyl chain and the cationic head group containing the boronic acid binding site. At highly hydrophobic surfaces such as that of the HOPG electrode spontaneous and reproducible monolayer formation is possible.

The voltammetric response for the reduction of alizarin red S in the presence of the boronic acid film (see Fig. 1B) is observed with a considerable peak-to-peak separation of *ca.* 0.37 V and a midpoint potential $E_{mid} = ½ (E_p^{ox} + E_p^{red}) = 0.54$ V *vs.* SCE. The midpoint potential is shifted positive when compared to the reduction of adsorbed alizarin red S in the absence of boronic acid, presumably due to the electron-withdrawing effect of the pyridinium boronic acid. In order to obtain additional information about the effect of the *N*-hexadecyl-pyridinium-4-boronic acid monolayer on the rate of interfacial electron transfer, experiments were conducted at a range of different scan rates. Fig. 2A shows a typical set of voltammograms and Fig. 2B summarises the effect of scan rate on peak current and peak potentials.

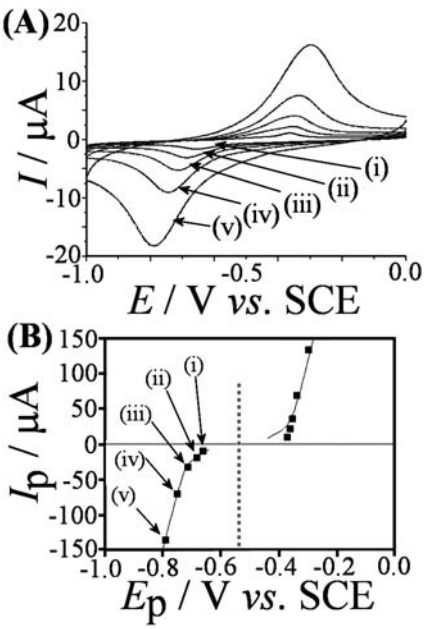

Fig. 2 (A) Cyclic voltammograms (scan rates (i) 0.02, (ii) 0.05, (iii) 0.1, (iv) 0.2, and (v) 0.5 V s^{-1}) for alizarin red S (adsorbed from 1 mM solution in aqueous 0.1 M phosphate buffer pH 7) at a 4.9 mm diameter basal plane HOPG electrode with 1 nmol *N*-hexadecyl-pyridinium-4-boronic acid hexafluorophosphate immobilised and immersed in 0.1 M phosphate buffer pH 7. (B) Plot of the peak current *versus* peak potential for reduction and re-oxidation and for a range of scan rates. The solid line corresponds to simulation data (DigiSim) for a 1 nm thin film of redox active molecules with two consecutive one-electron transfers with a standard rate constant $k_s = 10^{-10}$ m s^{-1}.

It can be seen that the increase in scan rate causes a further increase in the peak-to-peak separation. In order to quantify this effect a DigiSim simulation based on two consecutive one-electron transfer processes is employed. Thin film conditions are employed (1 nm thickness, chosen tentatively) to represent the adsorbed alizarin red S redox system and a heterogeneous standard rate constant of 10^{-10} m s^{-1} (see solid line in Fig. 2B) can be seen to closely reproduce the peak positions for the reduction process. For the re-oxidation and at low scan rates, the match of simulation and experimental data is not satisfactory probably due to additional complication such as a chemical step involving deprotonation. A good match of simulation and experiment confirms that slow electron transfer across the *N*-hexadecyl-pyridinium-4-boronic acid monolayer is responsible for the observed peak-to-peak separation. The corresponding standard heterogeneous rate constant for the adsorbed alizarin red S layer can be estimated as $k_{s,immobilised} = 10^{-10}$ m $s^{-1}/10^{-9}$ $m = 0.1$ s^{-1} which is in agreement for example with literature rate constant data for electron transfer to immobilised redox systems observed at catechol monolayer coated carbon surfaces.[47] Alternatively, it is possible to employ Laviron's expressions[48] for slow electron transfer in immobilised redox systems (see eqn (5) for reduction and eqn (6) for oxidation) to obtain mechanistic information. A comparison of experimental and theoretical data for peak potential *versus* logarithm of scan rate (not shown) is consistent with the above mechanism (the first electron transfer is rate limiting and therefore $n = 1$, the transfer coefficient is approximately $\alpha \approx 0.5$, and the standard rate constant is $k_{s,immobilised} \approx 0.1$ s^{-1}. In the equations R is the gas constant, T is the absolute temperature, F is the Faraday constant, $E_{p,c}$ and $E_{p,a}$ are the cathodic and anodic peak potentials, E'^0 is the formal potential, and v denotes the scan rate.

$$E_{p,c} = E'^0 - \frac{RT}{\alpha nF}\ln\left(\frac{\alpha nFv}{RTk_{s,immobilised}}\right) \quad (5)$$

$$E_{p,a} = E'^0 + \frac{RT}{(1-\alpha)nF}\ln\left(\frac{(1-\alpha)nFv}{RTk_{s,immobilised}}\right) \quad (6)$$

Next, the effect of the alizarin red S concentration during the binding process was investigated. Fig. 3A shows voltammograms obtained for alizarin red S concentrations from 1 μM to 1 mM and the plot in Fig. 3B demonstrates approximate agreement with a Langmuirian binding process with $K = 1.3 \times 10^5$ M^{-1}. The transition from unbound to bound state appears to be slightly more steep in the experimental data when compared to the theory indicating some attractive interaction of alizarin red S molecules when bound to the boronic acid film. Analysis of alizarin red S binding as a function of solution pH (during the adsorption step) (see Fig. 3C) is consistent with an only slight trend towards weaker binding for more acidic or more alkaline solutions and with a maximum at pH 5. The absence of a more pronounced effect of pH may be attributed to a binding mechanism with significant contributions from electrostatic, dispersion, and covalent forces (*vide infra*). Attempts to replace alizarin red S with analyte molecules such as fructose and glucose failed even with high concentrations and this may be attributed to a strong binding between alizarin red S and the *N*-hexadecyl-pyridinium-4-boronic acid hexafluorophosphate monolayer

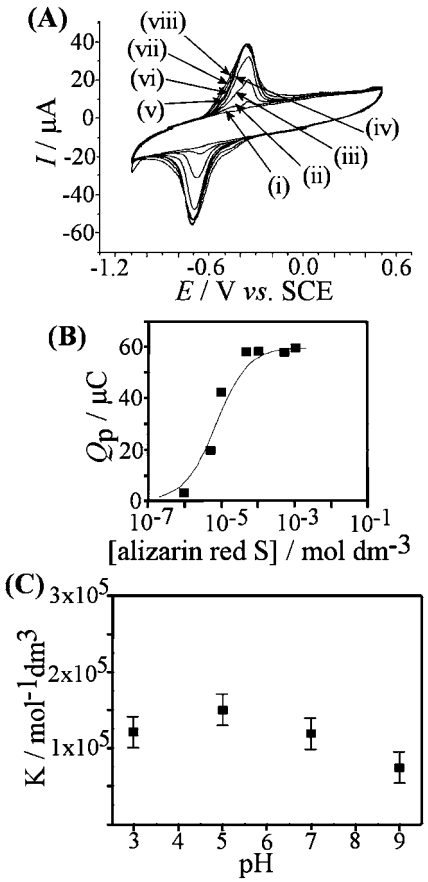

Fig. 3 (A) Cyclic voltammograms (scan rate 0.1 V s^{-1}) for alizarin red S (adsorbed from (i) 0, (ii) 1×10^{-6}, (iii) 5×10^{-6}, (iv) 1×10^{-5}, (v) 5×10^{-5}, (vi) 1×10^{-4}, (vii) 5×10^{-4}, and (viii) 1 mM solution in aqueous 0.1 M phosphate buffer pH 7) at a 4.9 mm diameter basal plane HOPG electrode with 1 nmol *N*-hexadecyl-pyridinium-4-boronic acid hexafluorophosphate immobilised immersed in 0.1 M phosphate buffer pH 7. (B) Plot of the charge under the reduction peak *versus* the concentration of alizarin red S during adsorption (the solid line shows Langmuirian binding with $K = 1.3 \times 10^5$ M^{-1}). (C) Plot of the Langmuirian binding constant *versus* pH during adsorption (with estimated errors).

which may be due again to a combination of factors including (i) binding to the boronic acid, (ii) electrostatic interactions, and (iii) hydrophobic interactions of alizarin red S with the modified electrode surface.

3.2. *N*-hexadecyl-pyridinium-4-boronic acid monolayer films II: binding of and anodic detection of catechols

Voltammetric data in Fig. 1A and B demonstrate that the oxidation of the catechol functional group of alizarin red S is suppressed after binding to the boronic acid film. However, this oxidation is only shifted to more positive potentials and it can be employed for analytical purposes. In contrast to the reduction of alizarin red S the oxidation is liberating the boronic acid bound molecule due to the transformation of the catechol to an *ortho*-diquinone. Therefore the *N*-hexadecyl-pyridinium-4-boronic acid hexafluorophosphate monolayer modified electrode can be employed for a much wider range of catechol analytes.

Voltammetry experiments conducted with a *N*-hexadecyl-pyridinium-4-boronic acid hexafluorophosphate monolayer modified basal plane HOPG electrode immersed in aqueous 0.1 M phosphate buffer solution in the presence of dopamine are shown in Fig. 4A. A partially reversible process indicating dopamine oxidation for dopamine in the solution phase is observed at a potential of *ca.* 0.15 V *vs.* SCE (see P3, eqn (7)).

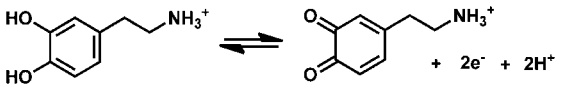

(7)

An additional oxidation response with higher sensitivity at lower dopamine concentration is observed at *ca.* 0.66 V *vs.* SCE (see P4, eqn (8)).

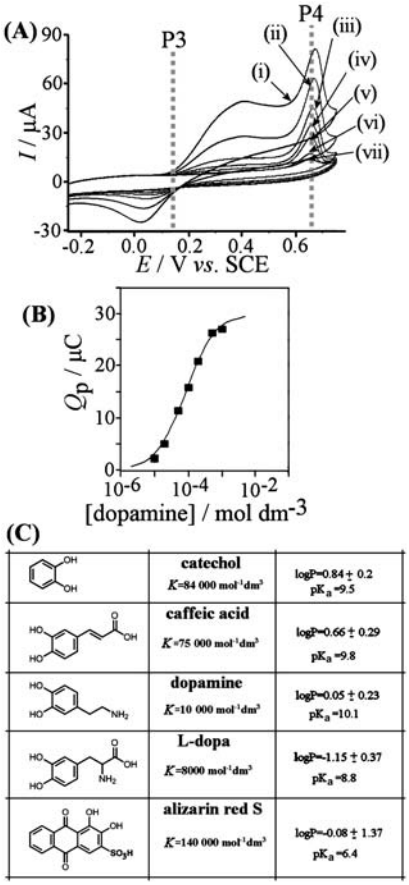

Fig. 4 (A) Cyclic voltammograms (scan rate 0.1 V s^{-1}) for the oxidation of dopamine at a 4.9 mm diameter basal plane HOPG electrode with 1 nmol *N*-hexadecyl-pyridinium-4-boronic acid hexafluorophosphate immobilised and immersed into aqueous 0.1 M phosphate buffer containing (i) 1×10^{-5}, (ii) 2×10^{-5}, (iii) 5×10^{-5}, (iv) 1×10^{-4}, (v) 2×10^{-4}, (vi) 5×10^{-4}, and (vii) 1×10^{-3} dopamine. (B) Plot of the charge under the dopamine oxidation peak P4 *versus* dopamine concentration. Solid line indicating Langmuirian binding with $K = 10^4$ M^{-1}. (C) Table of Langmuirian binding constants *K* for catechols. Also shown are log *P* estimates and the first pK_a for the hydroxyl proton based on ACDlab estimates.[49]

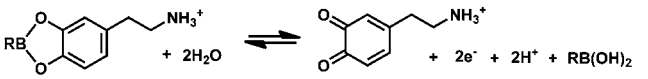

(8)

The shape of the oxidation peak P4 is characteristic for a surface immobilised redox system and the fact that the process is chemically irreversible is consistent with the oxidative removal of bound dopamine during the oxidation. However, the adsorbed layer quickly reforms and voltammetric analysis is possible without removal of the sensor from the analyte solution. The *N*-hexadecyl-pyridinium-4-boronic acid hexafluorophosphate monolayer is stable over many potential cycles. However, a further oxidation process at potential positive of 0.8 V *vs.* SCE (not shown) occurs which destroys the boronic acid film irreversibly most likely *via* oxidative C–B bond cleavage.

The analysis of the charge under the oxidation peak P4 *versus* the dopamine concentration is shown in Fig. 4B. Again a Langmuirian binding curve can be employed to extract an approximate binding constant of $K = 10^4$ M^{-1}. This binding constant is considerably lower compared to that obtained for alizarin red S and therefore a range of catechols was investigated. Fig. 4C shows a table summarising binding constant data for catechol, caffeic acid, dopamine, L-dopa, and alizarin red S. The strongest binding constant is observed for alizarin red S followed by catechol and caffeic acid. L-Dopa and dopamine show only weaker binding.

Attempts to correlate the binding constants with hydrophobicity (log *P* values) or with the acidity of the first hydroxyl (pK_a values) were not successful. The more hydrophilic nature and the positively charged amine functional groups on dopamine and L-dopa as well as the combination of molecular charge and hydrophobicity are likely to play a major and varying role in this selectivity sequence.

4. Conclusions

It has been shown that *N*-hexadecyl-pyridinium-4-boronic acid hexafluorophosphate can be readily deposited on basal plane HOPG as a monolayer with boronic acid functional groups. The amphiphilic nature of the molecule and the favourable interaction of the hexadecyl alkyl chain with the hydrophobic graphite substrate are responsible for this effect. Binding to the boronic acid monolayer is demonstrated for alizarin red S and for a range of catechol derivatives. Langmuirian binding is observed with a strong preference for negatively charge hydrophobic molecules such as alizarin red S. In future *N*-hexadecyl-pyridinium-4-boronic acid hexafluorophosphate monolayer can be employed on different types of sensor surfaces and *in situ* for the determination of dopamine or L-dopa directly in complex aqueous sample solutions.

Acknowledgements

Y-JH wishes to acknowledge University of Bath for the opportunity to carry out research in the TDJ group and China Scholarship Council for the grant supporting the visit. We would also like to thank the CAtalysis and SEnsing for our Environment (CASE) Network and CASE08 (Bath) and CASE09

(ECUST) for providing an environment where the basic ideas for this research were discussed and developed.

References

1 J. M. Sugihara and C. M. Bowman, *J. Am. Chem. Soc.*, 1958, **80**, 2443–2446.
2 J. P. Lorand and J. O. Edwards, *J. Org. Chem.*, 1959, **24**, 769–774.
3 B. Fabre and L. Taillebois, *Chem. Commun.*, 2003, 2982–2983.
4 L. Zhang, J. A. Kerszulis, R. J. Clark, T. Ye and L. Zhu, *Chem. Commun.*, 2009, 2151–2153.
5 V. E. Mouchrek, A. L. B. Marques, J. J. Zhang and G. O. Chierice, *Electroanalysis*, 1999, **11**, 1130–1136.
6 C. Berggren, P. Stalhandske, J. Brundell and G. Johansson, *Electroanalysis*, 1999, **11**, 156–160.
7 X. Y. Sun, B. Liu and Y. B. Jiang, *Anal. Chim. Acta*, 2004, **515**, 285–290.
8 M. J. Bonne, E. Galbraith, T. D. James, M. J. Wasbrough, K. J. Edler, A. T. A. Jenkins, M. Helton, A. McKee, W. Thielemans, E. Psillakis and F. Marken, *J. Mater. Chem.*, 2010, **20**, 588–594.
9 N. Katif, R. A. Harries, A. M. Kelly, J. S. Fossey, T. D. James and F. Marken, *J. Solid State Electrochem.*, 2009, **13**, 1475–1482.
10 X. Zhong, H. J. Bai, J. J. Xu, H. Y. Chen and Y. H. Zhu, *Adv. Funct. Mater.*, 2010, **20**, 992–999.
11 S. R. Ali, R. R. Parajuli, Y. Balogun, Y. F. Ma and H. X. He, *Sensors*, 2008, **8**, 8423–8452.
12 B. A. Deore, I. Yu, J. Woodmass and M. S. Freund, *Macromol. Chem. Phys.*, 2008, **209**, 1094–1105.
13 E. Granot, R. Tel-Vered, O. Lioubashevski and I. Willner, *Adv. Funct. Mater.*, 2008, **18**, 478–484.
14 X. T. Zhang, Y. F. Wu, Y. F. Tu and S. Q. Liu, *Analyst*, 2008, **133**, 485–492.
15 R. K. Shervedani and M. Bagherzadeh, *Electroanalysis*, 2008, **20**, 550–557.
16 M. Tanaka, R. Fujita and H. Nishide, *J. Nanosci. Nanotechnol.*, 2009, **9**, 634–639.
17 R. Polsky, J. C. Harper, D. R. Wheeler, D. C. Arango and S. M. Brozik, *Angew. Chem., Int. Ed.*, 2008, **47**, 2631–2634.
18 M. Shao and Y. Zhao, *Tetrahedron Lett.*, 2010, **51**, 2508–2511.
19 S. Q. Liu, B. Miller and A. C. Chen, *Electrochem. Commun.*, 2005, **7**, 1232–1236.
20 T. D. James, K. R. A. S. Sandanayake and S. Shinkai, *Angew. Chem., Int. Ed. Engl.*, 1994, **33**, 2207–2209.
21 T. D. James, K. R. A. S. Sandanayake, R. Iguchi and S. Shinkai, *J. Am. Chem. Soc.*, 1995, **117**, 8982–8987.
22 A. Matsumoto, K. Yamamoto, R. Yoshida, K. Kataoka, T. Aoyagi and Y. Miyahara, *Chem. Commun.*, 2010, **46**, 2203–2205.
23 T. D. James, K. R. A. S. Sandanayake and S. Shinkai, *J. Chem. Soc., Chem. Commun.*, 1994, 477–478.
24 T. D. James, P. Linnane and S. Shinkai, *Chem. Commun.*, 1996, 281–288.
25 T. D. James, K. R. A. S. Sandanayake and S. Shinkai, *Angew. Chem., Int. Ed. Engl.*, 1996, **35**, 1910–1922.
26 S. Arimori, M. L. Bell, C. S. Oh, K. A. Frimat and T. D. James, *Chem. Commun.*, 2001, 1836–1837.
27 S. Arimori, M. L. Bell, C. S. Oh, K. A. Frimat and T. D. James, *J. Chem. Soc., Perkin Trans. 1*, 2002, 803–808.
28 T. D. James and S. Shinkai, *Top. Curr. Chem.*, 2002, **218**, 159–200.
29 T. D. James, M. D. Phillips and S. Shinkai, *Boronic Acids in Saccharide Recognition*, RSC Publishing, The Royal Society of Chemistry, Cambridge, 2006.
30 T. D. James, *Top. Curr. Chem.*, 2007, **277**, 107–152.
31 T. R. Jackson, J. S. Springall, D. Rogalle, N. Masurnoto, H. C. Li, F. D'Hooge, S. P. Perera, A. T. A. Jenkins, T. D. James, J. S. Fossey and J. M. H. van den Elsen, *Electrophoresis*, 2008, **29**, 4185–4191.
32 D. K. Scrafton, J. E. Taylor, M. F. Mahon, J. S. Fossey and T. D. James, *J. Org. Chem.*, 2008, **73**, 2871–2874.
33 W. M. J. Ma, M. P. P. Morais, F. D'Hooge, J. M. H. van den Elsen, J. P. L. Cox, T. D. James and J. S. Fossey, *Chem. Commun.*, 2009, 532–534.
34 X. Yang, C. Dai, A. D. C. Molina and B. Wang, *Chem. Commun.*, 2010, **46**, 1073–1075.
35 M. P. P. Morais, J. D. Mackay, S. K. Bhamra, J. G. Buchanan, T. D. James, J. S. Fossey and J. M. H. van den Elsen, *Proteomics*, 2010, **10**, 48–58.
36 T. D. James, K. R. A. S. Sandanayake and S. Shinkai, *Nature*, 1995, **374**, 345–347.
37 J. Zhao, M. G. Davidson, M. F. Mahon, G. Kociok-Köhn and T. D. James, *J. Am. Chem. Soc.*, 2004, **126**, 16179–16186.
38 J. Z. Zhao, T. M. Fyles and T. D. James, *Angew. Chem., Int. Ed.*, 2004, **43**, 3461–3464.
39 J. Z. Zhao and T. D. James, *J. Mater. Chem.*, 2005, **15**, 2896–2901.
40 J. Z. Zhao and T. D. James, *Chem. Commun.*, 2005, 1889–1891.
41 L. Chi, J. Z. Zhao and T. D. James, *J. Org. Chem.*, 2008, **73**, 4684–4687.
42 F. Han, L. N. Chi, X. F. Liang, S. M. Ji, S. S. Liu, F. K. Zhou, Y. B. Wu, K. L. Han, J. Z. Zhao and T. D. James, *J. Org. Chem.*, 2009, **74**, 1333–1336.
43 X. Zhang, L. N. Chi, S. M. Ji, Y. B. Wu, P. Song, K. L. Han, H. M. Guo, T. D. James and J. Z. Zhao, *J. Am. Chem. Soc.*, 2009, **131**, 17452–17463.
44 X. Zhang, Y. B. Wu, S. M. Ji, H. M. Guo, P. Song, K. L. Han, W. T. Wu, W. H. Wu, T. D. James and J. Z. Zhao, *J. Org. Chem.*, 2010, **75**, 2578–2588.
45 A. Sikora, J. Zielonka, M. Lopez, J. Joseph and B. Kalyanaraman, *Free Radical Biol. Med.*, 2009, **47**, 1401–1407.
46 L. K. Mohler and A. W. Czarnik, *J. Am. Chem. Soc.*, 1993, **115**, 2998–2999.
47 N. H. Nguyen, C. Esnault, F. Gohier, D. Belanger and C. Cougnon, *Langmuir*, 2009, **25**, 3504–3508.
48 E. Laviron, *J. Electroanal. Chem.*, 1979, **101**, 19–28.
49 ACD/Labs, Advanced Chemistry Development Inc., Toronto, Canada, 2009, http://www.acdlabs.com.

